Synthesis of PS/Ag Nanocomposite Spheres with Catalytic and Antibacterial Activities

ARTICLE *in* ACS APPLIED MATERIALS & INTERFACES · SEPTEMBER 2012

Impact Factor: 6.72 · DOI: 10.1021/am3015313 · Source: PubMed

8 AUTHORS, INCLUDING:

Bo Peng
Utrecht University
23 PUBLICATIONS **236** CITATIONS
SEE PROFILE

pujun jin
Shaanxi Normal University
11 PUBLICATIONS **53** CITATIONS
SEE PROFILE

ACS APPLIED MATERIALS & INTERFACES

Research Article

www.acsami.org

Synthesis of PS/Ag Nanocomposite Spheres with Catalytic and Antibacterial Activities

Ziwei Deng,*[,†,‡] Haibao Zhu,[†,§] Bo Peng,[⊥] Hong Chen,[‡] Yuanfang Sun,[‡] Xiaodong Gang,[‡] Pujun Jin,[‡] and Juanli Wang[‡]

[‡]School of Materials Science and Engineering, Shaanxi Normal University, Xi'an, 710062, China

[§]College of Veterinary Medicine, Huazhong Agricultural University, Wuhan, 430070, China

[⊥]Soft Condensed Matter, Debye Institute for Nanomaterials Science, Utrecht University, Princetonplein 1, 3584 CC, Utrecht, The Netherlands

Supporting Information

ABSTRACT: This paper describes a simple, mild, and environmentally friendly approach to synthesize polystyrene/Ag (PS/Ag) nanocomposite spheres, which makes use of both reducing and stabilizing functions of polyvinylpyrrolidone (PVP) in aqueous media. In this approach, monodisperse polystyrene (PS) spheres, which are used as templates for the synthesis of core−shell nanocomposite spheres, are sulfonated first. Then, $[Ag(NH_3)_2]^+$ ions are adsorbed onto the surface of the PS template spheres via electrostatic attraction between $-SO_3H$ groups (grafted on the surface of the PS template spheres) and $[Ag(NH_3)_2]^+$ ions. $[Ag(NH_3)_2]^+$ ions are then reduced by and simultaneously protected by PVP. In this way, the PS/Ag nanocomposite spheres in aqueous media are obtained through a so-called one-pot method. Neither additional reducing agents nor toxic organic solvents are utilized during the synthesis process. Furthermore, the coverage degree and the particle size of Ag nanoparticles on PS/Ag nanocomposite spheres is easily tuned by changing the concentration of $[Ag(NH_3)_2]^+$ ions in aqueous media. Moreover, these PS/Ag nanocomposite spheres can be used as catalyst for the reduction of organic dyes and as antibacterial agents against *Salmonella* and *Escherichia coli*. In the present study, these PS/Ag nanocomposite spheres exhibit excellent catalytic properties (both in efficiency and recyclability) for the reduction of organic dyes, and the preliminary antibacterial assays indicate that these PS/Ag nanocomposite spheres also possess extraordinary antibacterial abilities against *Salmonella* and *Escherichia coli*.

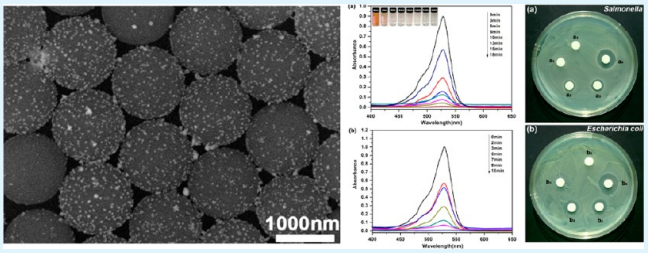

KEYWORDS: *polystyrene, silver, polyvinylpyrrolidone, nanocomposite spheres, catalysis, antibacterial activity*

INTRODUCTION

In recent years, nanostructured materials have attracted a comprehensive attention because of their novel physical, chemical, and biological properties and potential use in many applications,[1−4] especially those of metallic nanoparticles and their corresponding metal oxides, such as copper,[5,6] gold, silver,[7−11] zinc oxide,[12,13] and titanium oxide.[14−16] They have been commonly investigated as novel antimicrobial agents. Among them, silver is extensively used as an effective inhibitor, or a effective antimicrobial agent against different bacteria,[7,8] virus, and fungi,[17] with a minimal perturbation to human cells.[18,19] Unfortunately, the detailed role of silver as an antimicrobial mechanism is still not clearly understood, although it already proved itself as an excellent antibacterial agent for both environment and medical applications. Recent investigations suggested that Ag nanoparticles could react with sulfur-containing proteins inside or outside the cell membrane, which directly cause damage to the bacterial cell membrane and affect the viability of the bacterial cell.[8,20] Moreover, the Ag ions released from Ag nanoparticles can deactivate the micro-organism cells by destroying the replication process of cell membrane and DNA.[21,22]

Unlike ionic silver, the Ag nanoparticles significantly influence the antibacterial activity in varying dimensions. In principle, the smaller the particles, the better their antimicrobial performance. However, the aggregation of Ag nanoparticles, due to minimizing their surface energy, will lead to a loss of surface area and decreased antibacterial activity.[9,20,23] To overcome this shortcoming, many different approaches have been developed, mainly based on the incorporation of Ag nanoparticles into/onto various matrices.[24,25] For instance, polymer colloids,[26] inorganic oxides (such as silica,[27] titanium oxide,[28] and iron oxide[25]) have been commonly employed as substrates for Ag nanoparticles. A classic synthetic strategy of Ag nanocomposite spheres consists of two steps. First, activating the surface of template particles with the help of

Received: August 2, 2012
Accepted: September 19, 2012
Published: September 19, 2012

   dx.doi.org/10.1021/am3015313 | ACS Appl. Mater. Interfaces 2012, 4, 5625−5632

some compounds or metals such as $SnCl_2$,[29] gold[30] and palladium,[31] and second, coating Ag nanoparticles on the surface of these template particles. In addition, certain reducing agents (such as KBH_4, hydrazine, sodium citrate or ascorbic acid) must be applied in order to reduce silver precursors to metallic silver.[32,33] However, these compounds or reducing agents will remain as impurities in the final system, and potentially lead to a toxicity in environment or biological hazards. Therefore, an environmentally friendly method is highly desired.

Polyvinylpyrrolidone (PVP) has been demonstrated to be a good stabilizing agent for the preparation of monodisperse colloids in different species by our group[34−36] and other research groups.[37,38] It offers a unique combination of desired properties including chemical and biological inertness, and a low toxicity as well.[39] Recently, we demonstrated that PVP could be used as both reducing agent and stabilizing agent in the preparation of SiO_2/Ag composite spheres, wherein the $[Ag(NH_3)_2]^+$ ions were reduced to metallic nanoparticles by PVP, and the as-formed Ag nanoparticles were simultaneously protected by PVP. In our approach, neither additional reducing agents nor the surface modifications were necessary.[36] In this work, we inherit this facile method and extend it to decorate Ag nanoparticles onto the surface of polystyrene microspheres by utilizing the bifunctional agent (as reducing agent and stabilizer) of PVP in aqueous media. Our method is inherently an environmentally friendly method because of the absence of any toxic reagents. In addition, these PS/Ag nanocomposite spheres produced by this environmentally friendly method can be used as catalyst for the reduction of organic dyes or as antibacterial agents against *Salmonella* and *Escherichia coli*. These composite spheres exhibit a high efficiency and recyclability in catalysis, and an excellent antibacterial performance against *Salmonella* and *Escherichia coli* as well.

EXPERIMENTAL SECTION

Materials. Styrene was bought from Shanghai Chemical Reagent Co. (China) and the inhibitor was removed by vacuum distillation, and then stored at 4 °C. 2, 2′-azobisisobutyronitrile (AIBN) was purchased from Shanghai Chemical Reagent Co. (China) and purified by recrystallization in ethanol. Polyvinylpyrrolidone (PVP, M_W = 40 000 mol/g) was purchased from Sigma-Aldrich and used without further purification. Sulfuric acid (H_2SO_4, 98%), silver nitrate ($AgNO_3$, ≥99.8%), aqueous ammonia solution (28%), Rhodamine 6G, and absolute ethanol were purchased from Shanghai Chemical Reagent Co. (China) and used as received. Ultrapure water (>17 MΩ cm^{-1}) from a Milli-Q water system was used throughout the experiments.

Preparation of Monodisperse Polystyrene Spheres. Monodisperse polystyrene spheres (PS) were prepared by dispersion polymerization. In brief, all of styrene (15.0 g), PVP (3.0 g), AIBN (0.2 g), ethanol (95.0 g) and water (5.0 g) were added into a 250 mL four-necked round-bottom flask equipped with a mechanical stirrer, a thermometer with a temperature controller, a N_2 inlet, a Graham condenser and a heating mantle. The solution was deoxygenated by bubbling nitrogen gas at room temperature for ca. 60 min. Then, the reaction was heated to 70 °C and maintained for 24 h while stirring at 100 rpm. The obtained dispersion was centrifuged, washed with ethanol, and finally, dried in vacuum at room temperature for 24 h.

Preparation of Monodisperse Sulfonated Polystyrene Core−Shell Gel Spheres. These monodisperse PS spheres were sulfonated with the concentrated sulfuric acid, forming sulfonated PS core−shell gel spheres. The sulfonation process was described as follows:[35] In detail, dried PS powder (3.0 g) was dispersed into the concentrated sulfuric acid (98%, 30 mL) at 40 °C with a constant stirring rate at 100 rpm. After 4 h, the sulfonated PS core−shell gel spheres were obtained. They were separated by centrifugation, and washed with a large amount of ethanol several times, and then redispersed in the ultrapure water for subsequent use.

Preparation of PS/Ag Nanocomposite Spheres. The typical strategy to prepare PS/Ag nanocomposite spheres was based on our former reported method.[36] In brief, 10.0 g of dispersion containing 2.5 wt % of sulfonated PS core−shell gel spheres was mixed with 40 mL of PVP aqueous solution (5×10^{-4} mol/L). Then, 10 mL of a freshly prepared aqueous solution of $[Ag(NH_3)_2]^+$ (1.8×10^{-1} to 5.9×10^{-1} mol/L) was quickly added into the dispersion mentioned above, magnetically stirred at a speed of 100 rpm at room temperature for 1 h. Subsequently, this mixture was kept at 70 °C and stirred for around 7 h. The final products were collected by centrifugation, and several times washed with an excess amount of deionized water several times, and then redispersed in ultrapure water for further use.

Catalytic Activity of PS/Ag Nanocomposite Spheres. In a typical catalytic experiment, both dye (Rhodamine 6G, 2×10^{-5} mol/L) and KBH_4 (1×10^{-2} mol/L) were freshly prepared as aqueous solutions. Subsequently, a given amount of dispersion consisting of PS/Ag nanocomposite spheres was mixed with 10 mL of 2×10^{-5} mol/L Rhodamine 6G aqueous solution, and 1 mL of 1×10^{-2} mol/L KBH_4 solution was rapidly injected into this mixture while stirring. The color of the mixture was fading with the experiment proceeding, indicating a gradual reduction of Rhodamine 6G. The catalytic performance of PS/Ag nanocomposite spheres was studied by monitoring the variation in optical density at the wavelength of the absorbance maximum (λ_{max}) of the dye with a UV−vis.

Antibacterial Property. In the antibacterial tests, *Salmonella* (C79−13) and *Escherichia coli* (C83874) were used as the experimental strains, and Luria−Bertani (LB) medium was used for the growth of *Salmonella* and *Escherichia coli*. All disks and materials were sterilized in an autoclave before experiments. The antibacterial activities of PS/Ag nanocomposite spheres were measured by a paper disk diffusion assay according to the previous reports[40,41] on LB agar medium. The disk diffusion assay was performed by placing a 7 mm disk saturated by different amounts of PS/Ag nanocomposite spheres onto an agar plate seeded with *Salmonella* and *Escherichia coli*. Then, the diameters of the inhibition zones were measured after 24 h of incubation. To further examine the antibacterial abilities of PS/Ag nanocomposite spheres, 30 μL of *Salmonella* and *Escherichia coli* bacterial suspensions (O.D. = 0.6) were grown in 3 mL of liquid LB medium supplemented with different concentrations of PS/Ag nanocomposite spheres. The suspensions were shaken by a rotary shaker at 180 rpm at 37 °C, and their bacterial survivals were determined by measuring the optical density (O.D.) of LB in both medium at 600 nm after 24 h.

Characterization. *TEM Analysis.* Transmission electron microscopy (TEM, FEI Tecnai G20, USA FEI Corp.) was used to study the morphologies of obtained spheres (PS, sulfonated PS core−shell gel spheres and PS/Ag nanocomposite spheres). All dispersions were diluted with ethanol and sonicated at 25 °C for 10 min. Then, a droplet of dispersions was placed onto a carbon-coated copper grid and dried at room temperature before observation.

SEM Analysis. Scanning electron microscopy (SEM, FEI Quanta 200) was used to characterize the surface morphologies of PS, Sulfonated PS core−shell gel spheres, and PS/Ag nanocompsite spheres. All the sample dispersions were diluted with ethanol and dried on silica wafers at room temperature before observation.

EDX Analysis. An energy-dispersive X-ray spectroscopy (EDX) was conducted on the SEM to examine the surface composition of PS, Sulfonated PS core−shell gel spheres and PS/Ag nanocomposite spheres.

X-ray Diffraction. Powder X-ray diffraction was performed on a Rigaku Ultima IV powder diffractometer equipped with a Cu tube and a diffracted beam curved graphite monochromator operating at 40 kV and 44 mA. Crystal structure identification was carried out by scanning the sample powders supported on a glass substrate with a scanning rate of 0.02 degrees (2θ) per second in ranging from 30 to 90° (2θ).

UV−Visible Spectrum. UV−visible absorption spectra were recorded on a UV−visible Spectrophotometer. The samples were

placed in a 1 × 1 × 3 cm quartz cuvette, and the spectra were recorded at room temperature.

RESULTS AND DISCUSSION

Preparation and Characterization of PS/Ag Nanocomposite Spheres. The detailed preparation process of PS/Ag nanocomposite spheres has been illustrated in Scheme 1. In this approach, monodisperse PS spheres were used as templates and dispersed in concentrated sulfuric acid to sulfonate the surface of these PS spheres, leading to a core−shell structure. These core−shell particles were dispersed in a PVP aqueous solution after the last rinse. Then, a fresh $[Ag(NH_3)_2]^+$ aqueous solution was added into this sulfonated PS core−shell gel spheres dispersion. $[Ag(NH_3)_2]^+$ ions were easily adsorbed onto the surfaces of the sulfonated PS core−shell gel spheres via the electrostatic attraction between $-SO_3H$ groups and $[Ag(NH_3)_2]^+$ ions. In this case, PVP was used as a proper stabilizing agent to protect those sulfonated PS core−shell gel spheres from aggregation during the introduction of $[Ag(NH_3)_2]^+$ ions (If PVP was absent during the addition, a large amount of visible aggregations were formed). When the dispersion was heated to 70 °C and maintained for 7 h, $[Ag(NH_3)_2]^+$ ions were reduced and fixed at the surface of sulfonated PS core−shell gel spheres as Ag nanoparticles. Initially formed Ag nanoparticles served as seeds and could capture later reduced Ag. In the end, relatively big Ag nanoparticles were obtained and attached on the PS surface.

Scheme 1. Schematic Diagram Illustrating the Formation of PS/Ag Nanocomposite Spheres by Reduction and Stabilization of PVP in Aqueous Media

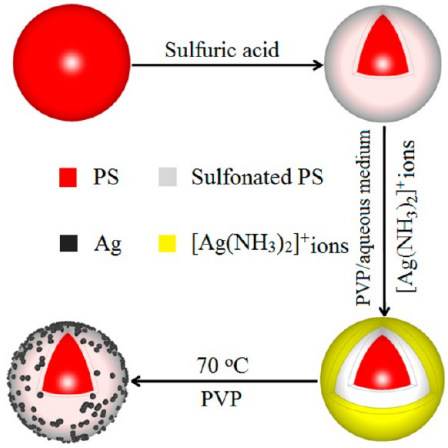

TEM and SEM images (see the Supporting Information, Figure S1) of original PS spheres prepared by dispersion polymerization indicate that PS spheres are monodisperse in size of 1.1 μm in diameter (by averaging 100 spheres in the TEM micrographs) with smooth surfaces. Therefore, these monodisperse PS spheres can be used as ideal templates for the formation of sulfonated PS core−shell gel spheres via sulfonation process in the concentrated sulfuric acid.[42,43] The morphology of the sulfonated PS core−shell gel spheres was examined by TEM (see Figure 1a), the results show that the sulfonation process does not have a significant influence on the average particle sizes and morphologies of PS spheres, because the sulfonation reaction usually occurs homogeneously at the surfaces of PS spheres.[42,43] Since in our previous work,[35] the existence of $-SO_3H$ groups in the sulfonated PS core−shell gel spheres has been confirmed with the FTIR spectrum, here, we are not repeating the measurement. In this way, these sulfonated PS core−shell gel spheres can be used as functional templates to form composite spheres with different shell compositions.[35,44,45]

Figure 1b displays a TEM image of PS/Ag nanocomposite spheres prepared by PVP in aqueous media. In comparison with the sulfonated PS core−shell gel spheres (Figure 1a), the composite spheres have relatively rough surfaces. High-magnification TEM images c and d in in Figure 1 clearly show the existence of Ag nanoparticles on the surfaces of sulfonated PS core−shell gel spheres.

Moreover, the morphologies of the sulfonated PS core−shell gel spheres before and after the coating of Ag nanoparticles are also examined by SEM (see Figure 2). Comparing the original sulfonated PS core−shell gel spheres in Figure 2a with the samples in Figure 2b, and combining their corresponding EDX spectra in panels c and d in Figure 2, respectively, Ag nanoparticles were found on the surfaces of the sulfonated PS core−shell particles after the coating process. Note, C and Si element signals in high intensity observed in the EDX spectra are originated from PS and silica wafer (Figure 2c). In addition, as shown in Figure 2d, the presence of Ag element signal can be observed in the EDX spectra of PS/Ag nanocomposite spheres. Therefore, these evidence demonstrate that PVP successfully

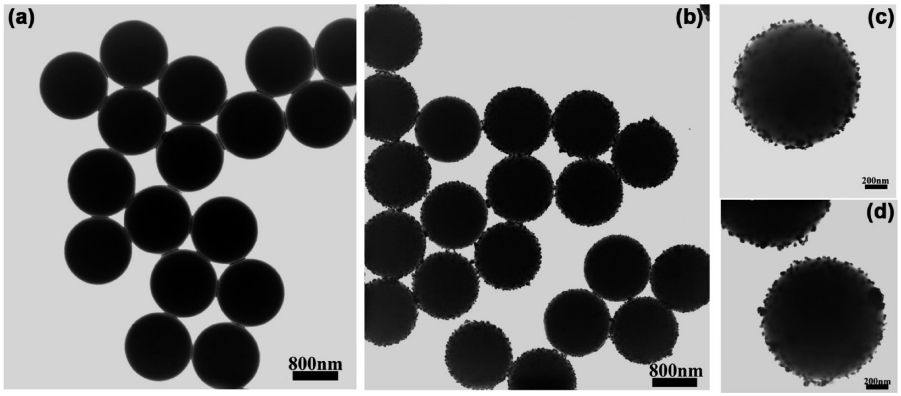

Figure 1. TEM images of (a) sulfonated PS core−shell gel spheres and (b) PS/Ag nanocomposite spheres prepared by PVP in aqueous media. (c) and (d) one typical PS/Ag nanocomposite sphere observed at high magnifications. Sulfonated PS core−shell gel spheres: 10.0 g (2.5 wt %); PVP: 5 × 10^{-4} mol/L; $[Ag(NH_3)_2]^+$ ions: 3.5 × 10^{-1} mol/L.

dx.doi.org/10.1021/am3015313 | ACS Appl. Mater. Interfaces 2012, 4, 5625−5632

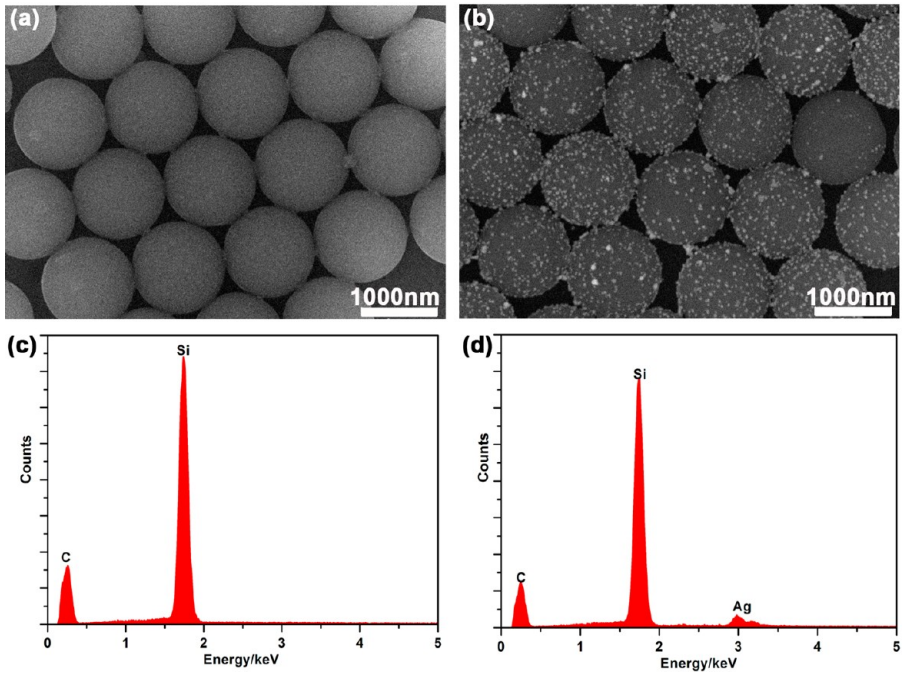

Figure 2. SEM images and the corresponding EDX spectra of (a, c) sulfonated PS core–shell gel spheres and (b, d) PS/Ag nanocomposite spheres prepared by PVP in aqueous media. Sulfonated PS core–shell gel spheres, 10.0 g (2.5 wt %); PVP, 5×10^{-4} mol/L; $[Ag(NH_3)_2]^+$ ions, 3.5×10^{-1} mol/L.

induce the reduction of $[Ag(NH_3)_2]^+$ ions to Ag nanoparticles. Meanwhile, PVP can also stabilize the system against aggregation in aqueous media.

In this process, $[Ag(NH_3)_2]^+$ ions are adsorbed onto the surfaces of the sulfonated PS core–shell gel spheres via electrostatic attraction between $-SO_3H$ groups and $[Ag(NH_3)_2]^+$ ions. No aggregates were found in all solutions, because PVP acts as a good stabilizing agent in aqueous media[2,36,46] to keep those sulfonated PS core–shell gel spheres in the presence of $[Ag(NH_3)_2]^+$ ions stable in all solutions. In addition, PVP takes the other function: the reduction of metal salts to metal nanoparticles in aqueous media. In fact, some groups have already demonstrated that PVP can act as a reducing agent successfully to reduce some noble metal (Au, Ag, Pd and Pt) salts to their noble metal nanoparticles in aqueous media.[47−49] However, publications in which makes use of the reductive property of PVP to prepare composite particles is scarce.[36]

X-ray Diffraction Patterns. The prepared PS/Ag nanocomposite spheres were dried in vacuum at room temperature for examination with XRD. The typical XRD patterns of the PS/Ag nanocomposite spheres have been illustrated in Figure 3, which exhibit the peaks at 2θ angles of 37.9, 44.1, 64.3, 77.2, and 81.4°, corresponding to the reflections of (111), (200), (220), (311), and (222) crystalline planes of the fcc structure of Ag (JCPDS No.04–0783), respectively. This indicates that the Ag nanocrystallites can be obtained through the reduction of $[Ag(NH_3)_2]^+$ ions with PVP.

Effect of the Concentrations of $[Ag(NH_3)_2]^+$ Ions. Figure 4 illustrates the SEM images of PS/Ag nanocomposite spheres prepared with different concentrations of $[Ag(NH_3)_2]^+$ ions. When the concentration of $[Ag(NH_3)_2]^+$ ions used in reaction solution was low, for example, 1.8×10^{-1} mol/L, only a small amount of Ag nanoparticles with low coverage was deposited on the surfaces of the sulfonated PS core–shell gel

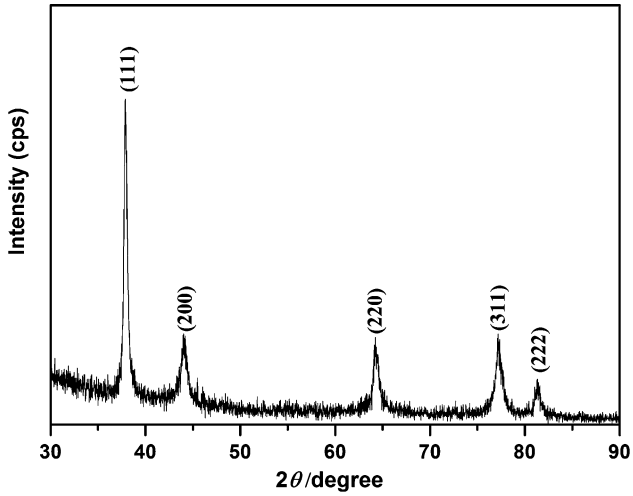

Figure 3. XRD patterns of PS/Ag nanocomposite spheres prepared by stabilization and reduction of PVP in aqueous media.

spheres (Figure 4a). As the concentration of $[Ag(NH_3)_2]^+$ ions increased to 3.5×10^{-1} mol/L, the amount of Ag nanoparticles loaded on the surfaces of sulfonated PS core–shell gel spheres was dramatically increased, as shown in Figure 4b. However, when further increased the content of $[Ag(NH_3)_2]^+$ ions in the reaction solution (e.g., 5.9×10^{-1} mol/L), some unbounded Ag nanoparticles can be observed on the silica wafer (Figure 4c). This result suggests that the sulfonated PS core–shell gel spheres are unable to absorb all the $[Ag(NH_3)_2]^+$ ions onto their surfaces via electrostatic attraction, a part of which remains in the aqueous media and are reduced by PVP. As a result, free Ag nanoparticles were present in this condition. It is worthwhile to point out that those free Ag nanoparticles are not aggregated (see Figure 4c), which also exhibits the high efficiency of the PVP as stabilizing agent in this system.

dx.doi.org/10.1021/am3015313 | ACS Appl. Mater. Interfaces 2012, 4, 5625–5632

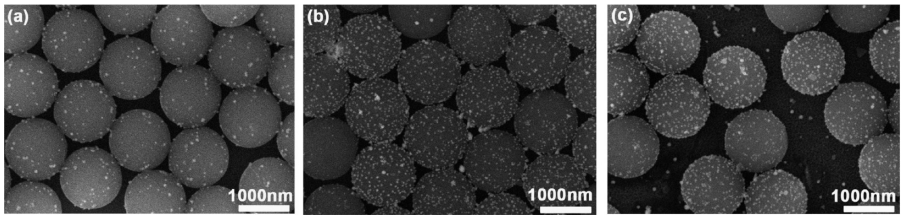

Figure 4. SEM images of PS/Ag nanocomposite spheres prepared by using various concentrations of $[Ag(NH_3)_2]^+$ ions, (a) 1.8×10^{-1} mol/L, (b) 3.5×10^{-1} mol/L, (c) 5.9×10^{-1} mol/L; sulfonated PS core–shell gel spheres, 10.0 g (2.5 wt %); PVP, 5×10^{-4} mol/L.

Moreover, the size of Ag nanoparticles has been measured from TEM and SEM images. With the concentrations of $[Ag(NH_3)_2]^+$ ions increase from 1.8×10^{-1} to 5.9×10^{-1} mol/L, the particle size of Ag nanoparticles on PS/Ag nanocomposite spheres increase from 41.5 to 58.3 nm accordingly, which indicates that the concentrations of $[Ag(NH_3)_2]^+$ ions can not only affect the coverage degree of Ag nanoparticles on PS/Ag nanocomposite spheres, but also the size of Ag nanoparticles.

In summary, these results demonstrate that the coverage degree and the particle size of Ag nanoparticles on the sulfonated PS core–shell gel spheres can be easily tuned through altering the concentration of the precursor-$[Ag(NH_3)_2]^+$ ions.

Catalytic Property of PS/Ag Nanocomposite Spheres. Metal nanoparticles have been extensively investigated for their catalytic activities for hydrogenation, hydroformylation, carbonylation, etc.[50−52] Unfortunately, in most cases, their catalytic abilities of these nanoparticles are reduced or even lost, when the coalescence of metal nanoparticles takes place. It is probably caused by van der Waals forces or high surface energy of nanoparticles if they are not protected. To solve this problem, we used PVP and sulfonated PS core–shell gel spheres as stabilizer and a support against the aggregation of Ag nanoparticles during and after the reduction reaction, respectively.

Generally, most of the organic dyes are synthetic compounds, which present a potential danger to the environment due to their toxicity and resistant to the aerobic degradation.[53,54] Herein, the catalytic degradation property of PS/Ag nanocomposite spheres for organic dyes is investigated. Rhodamine 6G is selected as a model dye and its evolution of UV–visible spectra at the wavelength of absorbance maximum (λ_{max}) during the reduction is illustrated in Figure 5. When the reaction system is in the presence of PS/Ag nanocomposite spheres (0.25 wt %), the absorbance at λ_{max} of Rhodamine 6G is quickly decreased with the reaction time (see Figure 5a). This can be directly reflected from the optical photos, in which the fading and ultimate bleaching of Rhodamine 6G solutions in color is appeared (see the inset in Figure 5a). With increasing the concentration of PS/Ag nanocomposite spheres in the reaction system, the reduction rate of Rhodamine 6G is increased (see Figure 5b). However, the absence of PS/Ag nanocomposite spheres (but in the presence of KBH_4) in the Rhodamine 6G solution only results in a slight decrease of λ_{max} after 24 h (see the Supporting Information, Figure S2). These results strongly indicate that the PS/Ag nanocomposite spheres have a very good catalytic performance.

For a catalyst, beside the catalytic efficiency, the recyclability of the catalyst is the other important factor in the judgment of this catalyst. In the measurement for the recyclability of these PS/Ag nanocomposite spheres a similar process was carried

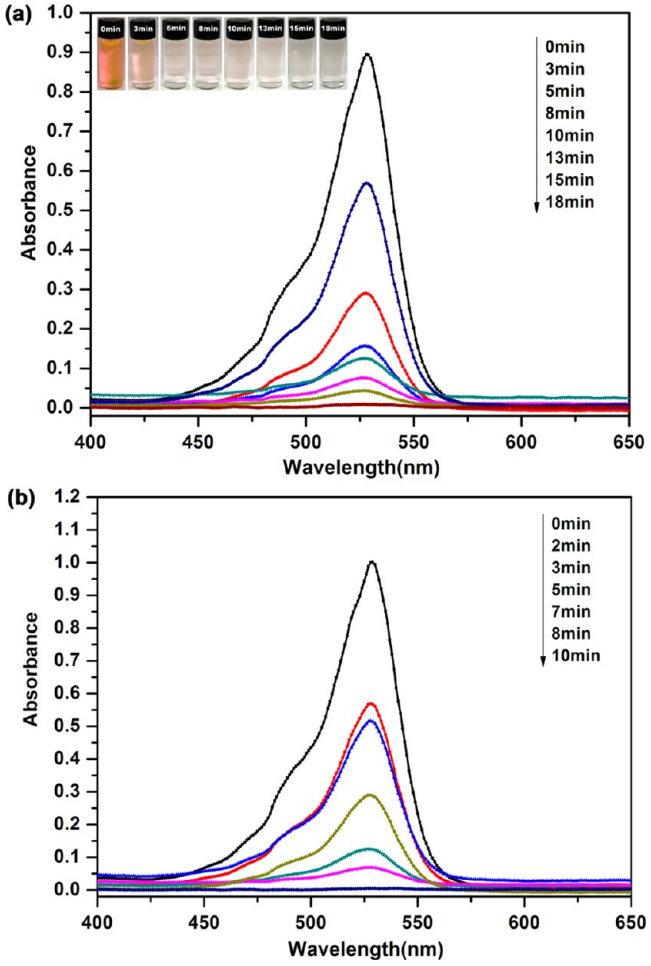

Figure 5. UV–visible spectra of Rhodamine 6G aqueous solution reduced by KBH_4 combined with PS/Ag nanocomposite spheres as functions of reaction time and the concentrations of PS/Ag nanocomposite spheres. PS/Ag nanocomposite spheres dispersions: (a) 0.25 wt % and (b) 0.5 wt %, 0.5 mL; Rhodamine 6G: 2×10^{-5} mol/L, 10 mL; KBH_4: 1×10^{-2} mol/L, 1 mL. The insets in a show the corresponding changes of Rhodamine 6G aqueous solutions in color.

out. In detail, 0.5 mL of dispersion containing 0.25 wt % of PS/Ag nanocomposite spheres was used to reduce 10 mL of a mixture in which Rhodamine 6G (2×10^{-5} mol/L) and KBH_4 (1×10^{-2} mol/L) were dissolved. After 18 min, PS/Ag nanocomposite spheres were collected by centrifuging, and then washed twice with deionized water. Finally, the particles redispersed in 0.5 mL deionized water for next cycle. After this procedure has been repeated six times, PS/Ag nanocomposite spheres were still stable and exhibited a high catalytic activity (the degradation efficiency was up to 89.8%), as shown in Figure 6. Therefore, the as-prepared PS/Ag nanocomposite

dx.doi.org/10.1021/am3015313 | ACS Appl. Mater. Interfaces 2012, 4, 5625−5632

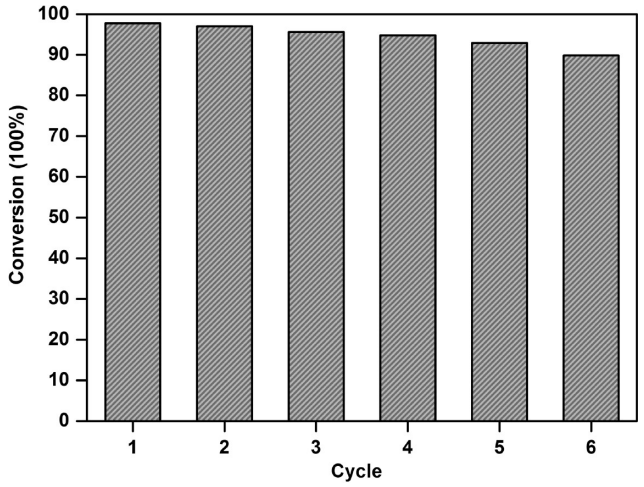

Figure 6. Recyclable catalytic ability of PS/Ag nanocomposite spheres as a catalyst for the reduction of Rhodamine 6G with KBH_4.

spheres are proven to be a potent recyclable catalyst. They could have a highly potential use in the degradation of the organic dyes in wastewater treatment applications.

Antibacterial Property of PS/Ag Nanocomposite Spheres. Silver and silver-based nanomaterials have been well-known for their strong inhibitory and antimicrobial effects.[23,55−57] Concerning the prospective applications of PS/Ag nanocomposite spheres as antibacterial materials, their antibacterial properties are evaluated with both *Salmonella* and *Escherichia coli* as bacterium models.

First, the antibacterial activities of PS/Ag nanocomposite spheres were investigated by measuring the growth inhibition of the bacteria on solid Luria−Bertani (LB) agar plates through a modified Kirby-Bauer method. In the disk diffusion assay experiment, the discs were saturated with different amounts of PS/Ag nanocomposite spheres, which were placed on LB agar plates and seeded with *Salmonella* and *Escherichia coli*. Subsequently, those plates are incubated at 37 °C for 24 h, and then the antibacterial effects in the form of inhibition zones are evaluated by measuring the disk diffusion assays. As shown in Figure 7, comparing with the blank control groups (Figure 7, a_0 and b_0), the zones of inhibition can be clearly observed in both *Salmonella* (Figure 7, a_1-a_4) and *Escherichia coli* (Figure 7, b_1−b_4) experimental groups. Moreover, with the concentrations of PS/Ag nanocomposite spheres increased gradually, the zone

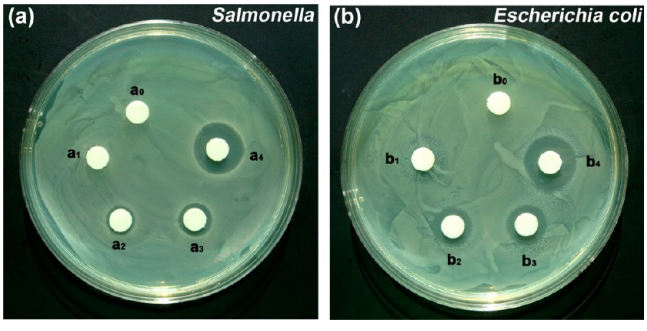

Figure 7. Inhibition zone test of as-synthesized PS/Ag nanocomposite spheres against *Salmonella* (a_0-a_4) and *Escherichia coli* (b_0−b_4). (a_0, b_0) Control groups, the ultrapure water are used as control. PS/Ag nanocomposite spheres: (a_1, b_1) 0.125 mg/mL; (a_2, b_2) 0.165 mg/mL; (a_3, b_3) 0.25 mg/mL; and (a_4, b_4) 0.5 mg/mL.

of inhibition grows. When the concentration of PS/Ag nanocomposite spheres is increased to 0.5 mg/mL, they exhibit a high antibacterial activity, which can be quantified by measuring the final diameters of inhibition zones at 18 and 19 mm for *Salmonella* and *Escherichia coli*, respectively. The details of the inhibition zone diameters for those samples against *Salmonella* and *Escherichia coli* are listed in Table1.

The Luria−Bertani (LB) liquid medium turbidity assays are also employed to evaluate the antibacterial activities of PS/Ag nanocomposite spheres against *Salmonella* and *Escherichia coli*. After the bacteria (*Salmonella* or *Escherichia coli*.) are cultured in the LB liquid media in the presence/or absence of the as-synthesized PS/Ag nanocomposite spheres for 24 h, their photographs of the mixture in tubes were taken and are shown in panels a and c in Figure 8. In the two control groups, the mixtures without PS/Ag nanocomposite spheres have become turbid after 24 h incubation, indicating that bacteria in such mixture media rapidly proliferated, whereas the media containing PS/Ag nanocomposite spheres (e.g., 0.5 mg/mL) remain pellucid (see Figure 8a, c), indicating that fewer bacteria proliferated. All results have qualitatively illustrated that PS/Ag nanocomposite spheres can inhibit *Salmonella* or *Escherichia coli* growth respectively, and the antibacterial activities mainly come from those Ag nanoparticles attached on the surfaces of PS spheres, because only pure sulfonated PS core−shell gel spheres cannot inhibit bacterial growth (see the Supporting Information, Figure S3).

On the other hand, we also quantitatively study the antibacterial activities of the synthesized PS/Ag nanocomposite spheres against *Salmonella* and *Escherichia coli*, that is, the investigation of the bacterial survival in LB liquid media after 24 h incubation. The bacterial survival can be monitored by the optical density at 600 (OD_{600}), and the survival rate of bacteria can be calculated as % survival = $A/B \times 100$ (where A is the number of surviving bacteria in the tested sample, and B is the number of surviving bacteria in the control group).[58] As shown in panels b and d in Figure 8, compared with those bacterial survivals in control groups, *Salmonella* and *Escherichia* bacterial survival in LB liquid media are only 9.6 and 5.5%, respectively, as they are treated by 0.5 mg/mL of PS/Ag nanocomposite spheres for 24 h incubation. Moreover, the results of bacterial survival with different concentrations of samples illustrate that the higher the PS/Ag nanocomposite sphere concentration, the better the antibacterial effects toward *Salmonella* or *Escherichia coli*, which is also consistent with that observed in disk diffusion assays.

CONCLUSIONS

In summary, we describe a simple, mild, and environmentally friendly method to fabricate PS/Ag nanocomposite spheres through utilizing the dual functions of PVP, that is, as reducing agent and stabilizing agent in aqueous media. Neither additional reducing agent nor toxic organic solvents are necessary in this process. TEM, SEM, and EDX results have confirmed the formation of PS/Ag nanocomposite spheres. In addition, the coverage degree and the particle size of Ag nanoparticles on the PS spheres can be easily tuned through varying the concentration of $[Ag(NH_3)_2]^+$ ions. XRD patterns indicate that the obtained Ag nanoparticles are crystalline. Moreover, PS/Ag nanocomposite spheres proved to have a good recyclable catalytic performance in the degradation of Rhodamine 6G. And the preliminary antibacterial assays indicate that these PS/Ag nanocomposite spheres possess

Table 1. Detailed Zone Diameters of the Inhibition Test Results for the Ps/Ag Nanocomposite Spheres against *Salmonella* and *Escherichia coli*

	initial diameter (mm)		final inhibition zone diameter (mm)		diffusion[b] (mm)	
sample (mg/mL)	*Salmonella*	*Escherichia coli*	*Salmonella*	*Escherichia coli*	*Salmonella*	*Escherichia coli*
control[a]	7	7	7	7	0	0
0.125	7	7	7	7	0	0
0.167	7	7	10	12	3	5
0.25	7	7	12	13	5	6
0.5	7	7	18	19	11	12

[a]The ultrapure water in absence of PS/Ag nanocomposite spheres is used in the control experiments. [b]Diffusion (nm) = final inhibition zone diameter (nm) − initial diameter (nm).

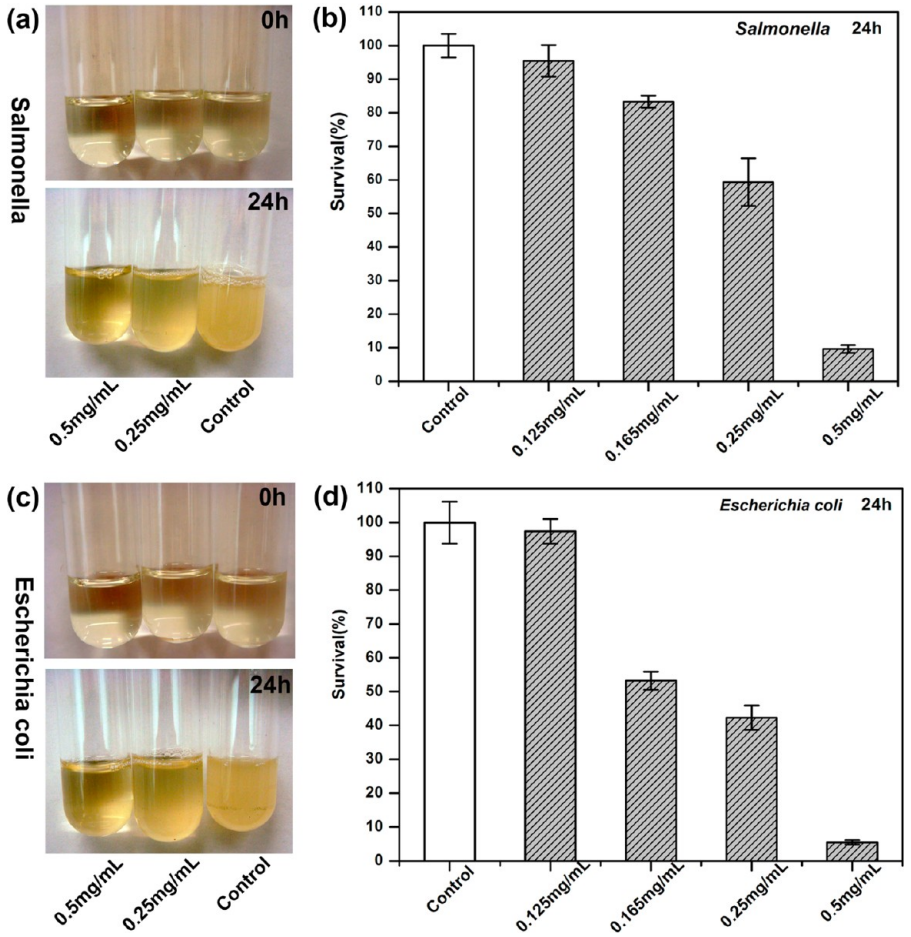

Figure 8. (a, c) LB liquid medium turbidity assays and the bacterial survival measurements; (b, d) are employed to evaluate antibacterial activities of PS/Ag nanocomposite spheres against *Salmonella* and *Escherichia coli*. (a, c) Bacteria in LB liquid medium containing 0.5 and 0.25 mg/mL of PS/Ag nanocomposite spheres are studied, respectively, and the ultrapure water is used in the control experiments. Photographs are taken at the beginning 0 h and after 24 h of incubation. (b, d) Different concentrations of PS/Ag nanocomposite spheres (0.125−0.5 mg/mL) are added to inhibit the culture of *Salmonella* and *Escherichia coli*. The bacterial survival is measured with the optical density at 600 nm wavelength.

excellent antibacterial abilities against *Salmonella* and *Escherichia coli*. Given these advantages, we believe these PS/Ag nanocomposite spheres can be broadly used as recyclable catalysts for reducing organic dyes in the wastewater treatment and as antibacterial agent for medical and environmental applications.

■ ASSOCIATED CONTENT

Ⓢ Supporting Information

TEM and SEM images of PS spheres prepared by dispersion polymerization, UV−visible spectra of Rhodamine 6G aqueous solutions mixed with KBH_4 aqueous solution in the absence of PS/Ag nanocomposite spheres, The bacterial survival measurement of sulfonated PS core−shell gel spheres against *Salmonella* and *Escherichia coli*. This material is available free of charge via the Internet at http://pubs.acs.org.

■ AUTHOR INFORMATION

Corresponding Author

*Tel:+86-29-81530804. Fax:+86-29-81530702. E-mail: zwdeng@snnu.edu.cn.

Author Contributions

[†]These two authors contributed equally to this work

Notes

The authors declare no competing financial interest.

■ ACKNOWLEDGMENTS

This research work is supported by the Fundamental Research Funds for the Central Universities (GK201102003). The authors thank Zhaofang Xi and Dongyang Liu (College of Veterinary Medicine, Huazhong Agricultural University, China) for supporting all the experimental bacteria in this research work, and A. J. van de Glind is thanked for critical reading of this paper.

■ REFERENCES

(1) Park, J.; Joo, J.; Kwon, S. G.; Jang, Y.; Hyeon, T. *Angew. Chem., Int. Ed.* **2007**, *46*, 4630−4660.
(2) Sun, Y. G.; Xia, Y. N. *Science* **2002**, *298*, 2176−2179.
(3) Nie, S. M.; Emery, S. R. *Science* **1997**, *275*, 1102−1106.
(4) Cao, Y. W. C.; Jin, R. C.; Mirkin, C. A. *Science* **2002**, *297*, 1536−1540.
(5) Bagihalli, G. B.; Avaji, P. G.; Patil, S. A.; Badami, P. S. *Eur. J. Med. Chem.* **2008**, *43*, 2639−2649.
(6) Kim, Y. H.; Lee, D. K.; Cha, H. G.; Kim, C. W.; Kang, Y. C.; Kang, Y. S. *J. Phys. Chem. B* **2006**, *110*, 24923−24928.
(7) Pal, S.; Tak, Y. K.; Song, J. M. *Appl. Environ. Microbiol.* **2007**, *73*, 1712−1720.
(8) Feng, Q. L.; Wu, J.; Chen, G. Q.; Cui, F. Z.; Kim, T. N.; Kim, J. O. *J. Biomed. Mater. Res.* **2000**, *52*, 662−668.
(9) Panacek, A.; Kvitek, L.; Prucek, R.; Kolar, M.; Vecerova, R.; Pizurova, N.; Sharma, V. K.; Nevecna, T.; Zboril, R. *J. Phys. Chem. B* **2006**, *110*, 16248−16253.
(10) Zhao, Y. Y.; Tian, Y.; Cui, Y.; Liu, W. W.; Ma, W. S.; Jiang, X. Y. *J. Am. Chem. Soc.* **2010**, *132*, 12349−12356.
(11) Arshi, N.; Ahmed, F.; Kumar, S.; Anwar, M. S.; Lu, J.; Koo, B. H.; Lee, C. G. *Curr.Appl.Phys.* **2011**, *11*, S360−S363.
(12) Applerot, G.; Lipovsky, A.; Dror, R.; Perkas, N.; Nitzan, Y.; Lubart, R.; Gedanken, A. *Adv. Funct. Mater.* **2009**, *19*, 842−852.
(13) Wang, X. L.; Yang, F.; Yang, W.; Yang, X. R. *Chem. Commun.* **2007**, *42*, 4419−4421.
(14) Heinlaan, M.; Ivask, A.; Blinova, I.; Dubourguier, H. C.; Kahru, A. *Chemosphere* **2008**, *71*, 1308−1316.
(15) Sunada, K.; Kikuchi, Y.; Hashimoto, K.; Fujishima, A. *Environ. Sci. Technol.* **1998**, *32*, 726−728.
(16) Adams, L. K.; Lyon, D. Y.; Alvarez, P. J. J. *Water Res.* **2006**, *40*, 3527−3532.
(17) Panyala, N. R.; Pena-Mendez, E. M.; Havel, J. *J. Appl. Biomed.* **2008**, *6*, 117−129.
(18) AshaRani, P. V.; Mun, G. L. K.; Hande, M. P.; Valiyaveettil, S. *ACS Nano* **2009**, *3*, 279−290.
(19) Bosetti, M.; Masse, A.; Tobin, E.; Cannas, M. *Biomaterials* **2002**, *23*, 887−892.
(20) Morones, J. R.; Elechiguerra, J. L.; Camacho, A.; Holt, K.; Kouri, J. B.; Ramirez, J. T.; Yacaman, M. J. *Nanotechnology* **2005**, *16*, 2346−2353.
(21) Matsumura, Y.; Yoshikata, K.; Kunisaki, S. i.; Tsuchido, T. *Appl. Environ. Microbiol.* **2003**, *69*, 4278−4281.
(22) Gupta, A.; Maynes, M.; Silver, S. *Appl. Environ. Microbiol.* **1998**, *64*, 5042−5045.
(23) Baker, C.; Pradhan, A.; Pakstis, L.; Pochan, D. J.; Shah, S. I. *J. Nanosci. Nanotechnol.* **2005**, *5*, 244−249.
(24) Sureshkumar, M.; Siswanto, D. Y.; Lee, C. K. *J. Mater. Chem.* **2010**, *20*, 6948−6955.
(25) aDallas, P.; Tucek, J.; Jancik, D.; Kolar, M.; Panacek, A.; Zboril, R. *Adv. Funct. Mater.* **2010**, *20*, 2347−2354.
(26) Chen, Z. M.; Gang, T.; Yan, X.; Li, X.; Zhang, J. H.; Wang, Y. F.; Chen, X.; Sun, Z. Q.; Zhang, K.; Zhao, B.; Yang, B. *Adv. Mater.* **2006**, *18*, 924−929.
(27) Caruso, F.; Spasova, M.; Saigueirino-Maceira, V.; Liz-Marzan, L. M. *Adv. Mater.* **2001**, *13*, 1090−1094.
(28) Necula, B. S.; Fratila-Apachitei, L. E.; Zaat, S. A. J.; Apachitei, I.; Duszczyk, J. *Acta Biomater.* **2009**, *5*, 3573−3580.
(29) Kobayashi, Y.; Salgueirino-Maceira, V.; Liz-Marzan, L. M. *Chem. Mater.* **2001**, *13*, 1630−1633.
(30) Jackson, J. B.; Halas, N. J. *J. Phys. Chem. B* **2001**, *105*, 2743−2746.
(31) Warshawsky, A.; Upson, D. A. *J. Polym. Sci., Part A: Polym. Chem.* **1989**, *27*, 2963−2994.
(32) Zhang, J. L.; Han, B. X.; Liu, J. C.; Zhang, X. G.; He, J.; Liu, Z. M.; Jiang, T.; Yang, G. Y. *Chem.—Eur. J.* **2002**, *8*, 3879−3883.
(33) Henglein, A.; Giersig, M. *J. Phys. Chem. B* **1999**, *103*, 9533−9539.
(34) Deng, Z. W.; Chen, M.; Zhou, S. X.; You, B.; Wu, L. M. *Langmuir* **2006**, *22*, 6403−6407.
(35) Deng, Z. W.; Chen, M.; Gu, G. X.; Wu, L. M. *J. Phys. Chem. B* **2008**, *112*, 16−22.
(36) Deng, Z. W.; Chen, M.; Wu, L. M. *J. Phys. Chem. C* **2007**, *111*, 11692−11698.
(37) Imhof, A. *Langmuir* **2001**, *17*, 3579−3585.
(38) Graf, C.; Vossen, D. L. J.; Imhof, A.; van Blaaderen, A. *Langmuir* **2003**, *19*, 6693−6700.
(39) Wessel, W.; Schoog, M.; Winkler, E. *Arzneim.-Forsch.* **1971**, *21*, 1468−1482.
(40) Conner, D. E.; Beuchat, L. R. *J. Food Sci.* **1984**, *49*, 429−434.
(41) Elgayyar, M.; Draughon, F. A.; Golden, D. A.; Mount, J. R. *J. Food Prot.* **2001**, *64*, 1019−1024.
(42) Yang, Z.; Li, D.; Rong, J.; Yan, W.; Niu, Z. *Macromol. Mater. Eng.* **2002**, *287*, 627−633.
(43) Yang, Z. Z.; Niu, Z. W.; Lu, Y. F.; Hu, Z. B.; Han, C. C. *Angew. Chem., Int. Ed.* **2003**, *42*, 1943−1945.
(44) Niu, Z. W.; Yang, Z. H.; Hu, Z. B.; Lu, Y. F.; Han, C. C. *Adv. Funct. Mater.* **2003**, *13*, 949−954.
(45) Wang, Z. X.; Chen, X. B.; Chen, M.; Wu, L. M. *Langmuir* **2009**, *25*, 7646−7651.
(46) Sun, Y. G.; Yin, Y. D.; Mayers, B. T.; Herricks, T.; Xia, Y. N. *Chem. Mater.* **2002**, *14*, 4736−4745.
(47) Hoppe, C. E.; Lazzari, M.; Pardiñas-Blanco, I.; López-Quintela, M. A. *Langmuir* **2006**, *22*, 7027−7034.
(48) Xiong, Y.; Washio, I.; Chen, J.; Cai, H.; Li, Z.; Xia, Y. *Langmuir* **2006**, *22*, 8563−8570.
(49) Washio, I.; Xiong, Y.; Yin, Y.; Xia, Y. *Adv. Mater.* **2006**, *18*, 1745−1749.
(50) Ahmadi, T. S.; Wang, Z. L.; Green, T. C.; Henglein, A.; El-Sayed, M. A. *Science* **1996**, *272*, 1924−1925.
(51) Pal, T.; Sau, T. K.; Jana, N. R. *Langmuir* **1997**, *13*, 1481−1485.
(52) Jiang, Z.; Liu, C.; Sun, L. *J. Phys. Chem. B* **2005**, *109*, 1730−1735.
(53) Stylidi, M.; Kondarides, D. I.; Verykios, X. E. *Appl. Catal. B: Environ.* **2003**, *40*, 271−286.
(54) Konstantinou, I. K.; Albanis, T. A. *Appl. Catal. B: Environ.* **2004**, *49*, 1−14.
(55) Kim, Y. H.; Kim, C. W.; Cha, H. G.; Lee, D. K.; Jo, B. K.; Ahn, G. W.; Hong, E. S.; Kim, J. C.; Kang, Y. S. *J. Phys. Chem. C* **2009**, *113*, 5105−5110.
(56) Kim, Y. H.; Lee, D. K.; Cha, H. G.; Kim, C. W.; Kang, Y. S. *J. Phys. Chem. C* **2007**, *111*, 3629−3635.
(57) Lv, M.; Su, S.; He, Y.; Huang, Q.; Hu, W. B.; Li, D.; Fan, C. H.; Lee, S. T. *Adv. Mater.* **2010**, *22*, 5463−5467.
(58) Bai, H. W.; Liu, Z. Y.; Sun, D. D. *Phys. Chem. Chem. Phys.* **2011**, *13*, 6205−6210.